DTU Library

Image Processing for daylight Electroluminescence PV Imaging acquired in movement

Benatto, Gisele Alves dos Reis; Mantel, Claire; Santamaria Lancia, Adrian Alejo; Graversen, Michael; Riedel, Nicholas; Thorsteinsson, Sune; Poulsen, Peter Behrensdorff; Forchhammer, Søren; Parikh, Harsh; Spataru, Sergiu

IMAGE PROCESSING FOR DAYLIGHT ELECTROLUMINESCENCE PV IMAGING ACQUIRED IN MOVEMENT

Gisele A. dos Reis Benatto[1], Claire Mantel[1], Adrian A. Santamaria Lancia[1], Michael Graversen[1]; Nicholas Riedel[1], Sune Thorsteinsson[1], Peter B. Poulsen[1], Søren Forchhammer[1], Harsh Parikh[2], Sergiu Spataru[2] and Dezso Sera[2]

[1] Department of Photonics Engineering, Technical University of Denmark, Frederiksborgvej 399, 4000, Roskilde, Denmark,
[2] Department of Energy Technology, Aalborg University, Pontoppidanstraede 101, 9220, Aalborg, Denmark.

ABSTRACT – Regular photovoltaic (PV) system inspections have become a challenge with the significant growth in the number of modules and peak power capacity of PV installations. Image acquisition using drones, based on visual, thermographic, and more recently luminescence, can be a viable solution for large-scale PV inspections. As luminescence can provide a highly detailed and accurate PV module failure diagnosis, the development of a daylight electroluminescence (EL) imaging capability is of high importance. EL imaging performed in the field during the day requires the enhancement of the relatively weak luminescence signal over the noise from the sun. This is accomplished by image averaging and background subtraction, which requires the highly accurate registering of the of individual module images. A sequential EL image acquisition at high frame rates in continuous motion at different angles will be the real-world situation for a drone-based PV inspection in daylight, and to account for this movement while maintaining high quality images, several image processing steps must be developed. With this motivation, here we describe and perform EL image processing on a module with different faults to assure quality of the EL images in different motion speeds.

Keywords: Daylight electroluminescence, Field inspections, Image processing.

1 INTRODUCTION

Imaging techniques such as infrared thermography (IRT) and electroluminescence (EL) are excellent tools for fault detection of both small and large-scale PV installations. At the same time, such inspections are highly important to ensure the expected return on investment (ROI). Drone-based IRT surveys of solar plants are a reality today, and are expected to become an automated inspection method in the near future [1]. The accuracy of thermographic fault detection though, presents limitations, which can be surpassed when performed in combination with EL imaging of the panels. EL can be used to rapidly and accurately detect a large range of major and minor faults in PV modules such as cell cracks, broken interconnections, potential induced degradation (PID) among others [2], [3]. State-of-the-art EL image acquisition however; faces crucial technical challenges, including long exposure times and low signal-to-noise ratio under sun irradiation.

The most commonly used cameras for EL have silicon-based sensors (such as CCD), which present a weak spectral sensitivity in the EL emission range of crystalline silicon (c-Si) solar cells. Although a high resolution (>10MP) can easily be achieved with these detectors, their required long exposure times (of the order of seconds) limit the inspection speed and their application in unmanned aerial vehicle (UAV). In contrast, cameras with InGaAs-based detectors have a good spectral response to the silicon luminescence emission and therefore short integration times, which can be as short as 1 µs [4].

While nighttime EL imaging presents few acquisition challenges, applying high power to PV strings can pose a safety risk to the operators and drone flights can be restricted by national and local laws for UAV night flights. To perform daylight EL in movement, the capability to acquire many images per scene, with high frame rates is essential to perform denoise by averaging and increase signal-to-noise ratio (SNR). No only for EL images, but high frame rates are needed for the obtainment of background images to remove ambient light, required even with the use of filters.

Together with the current efforts to build up a full automated solar plant inspection method including visual; IRT and EL in the future with UAVs [2], [5]–[7], here we describe and perform EL image processing on a module with different faults to insure quality of the EL images acquired in daylight and in movement.

2 EXPERIMENTAL DETAILS

2.1 Sample and electrical signal

For this experiment, a module of 36 multi-crystalline 15.6 x 15.6 cm cells arranged in a 6 x 6 cells matrix was prepared. This module was mechanically stressed and contained cells with several mode A, B and C cracks. The experiment was performed outdoors, under bright daylight with irradiance indicated in the results section. The module was installed facing south with correspondent global horizontal irradiance (GHI) and plane of array (POA) irradiance measured just before an image sequence acquisition using a silicon reference cell from ReRa Solutions connected to a multimeter.

For this outdoor EL setup, a new concept using an AC power supply unit (PSU) was tested. To perform daylight EL imaging, a modulated or lock-in electrical bias is required. In previous works, this modulation was performed by a modulation box synchronized with a camera trigger. This approach required additional hardware to control the power supply unit (PSU) signal and synchronize to camera. In contrast, the AC PSU used in this work (Keysight AC6804A) did not require the additional hardware for synchronization of the PSU and camera, and thus simplified

the ground-based system and avoided additional hardware attached to the camera. The forward bias applied to the PV consists of an AC+DC coupling signal (AC signal with a DC offset). The AC+DC electrical signal and applied to the PV module was monitored using a multiphase power analyzer (Tektronix PA4000) in a 4-wire configuration. The AC+DC sinusoidal signal frequency was 60 Hz, while image acquisition was performed with a frame rate of 120 Hz. These frequencies were chosen to accommodate the acquisition of the EL and background (BG) images (Fig. 1). The camera was not actively synchronized with the bias signal, therefore the mean of the pixel numbers of the frames was verified before image processing. We looked at the mean pixel values of the 16 bits image frames acquired in sequence during electrical modulation and compared the differences to determine when the image was EL (high mean) or BG (low mean). The frequencies of the electrical bias and framerate results in collecting an EL and background (BG) image one after the other. This approach avoids the interference of rapid fluctuations in solar irradiance due to different levels of cloud cover during the measurement, as it was verified in our tests that non-modulated EL and BG images acquisition do not offer the same level of image quality after denoising by averaging and EL/BG subtraction.
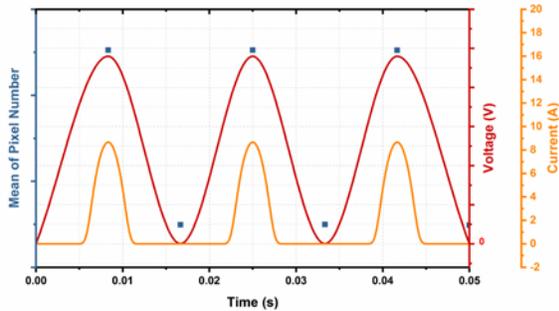
Figure 1: Electrical signal applied to the PV panel and mean of pixel numbers of the images acquired.

2.2 Testbed and moving camera

An InGaAs camera with 640x512 resolution and 14 bits dynamic range from Raptor Photonics is used for the experiment. A PC connected to the camera was required for image data acquisition and settings control. The EL videos were acquired at 120 frames per second (fps). To improve the SNR in the EL images, 16 to 50 EL/BG image pairs are required and the high frame rate allows obtaining this range of images in movement [7]. The exposure time was auto selected by the camera and kept fixed at 0.26 ms for the two image sequences presented here. This exposure time was adequate to avoid over or under exposure for the slightly different irradiances observed during the image sequences (775 W/m^2 and 761 W/m^2 GHI).

The luminescence emission peak for silicon-based solar cells at ambient temperature is centered around 1150 nm [8], therefore, to avoid detecting light from the sun and surroundings, an OD>4.0 1150 nm band-pass filter with 50nm FWHM was used. A 25 mm fixed focus sapphire lens

without aperture control was used, and in order to photograph the entire area of the panel, the camera was placed approximately four meters from the test string.

The camera tripod was fixed on a dolly, equipped with proper wheels to be placed over a rail (Fig. 2). This mount allowed the acquisition of EL images at a fixed distance from the PV module, while the camera moved in parallel along horizontally. The tripod was moved manually, permitting speeds of up to 2 m/s and regular speeds up to 1.5 m/s. The speed of the motion during image acquisition was calculated from the video/image sequence acquisition. Two different speeds were studied in similar irradiance conditions: 0.8 m/s (Speed 1) and 1.5 m/s (Speed 2).
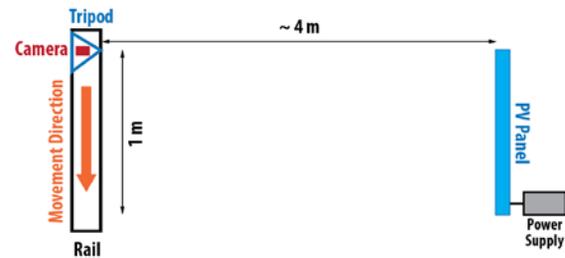

Figure 2: Test bed top view. The camera was mounted on a tripod over a rail to replicate the moviment performed by an UAV.

3   RESULTS

3.1 Image processing

While image processing for stationary EL corresponds to EL/BG image separation, averaging, BG subtraction and finally quality control, images acquired in movement add a much higher level of complexity to this process. At first, the acquired images had to be checked for motion blur. At 2 m/s no visible blur was detected by visual inspection.

The diagram of Fig. 3 shows the image processing steps performed in this work. The colors indicate high (red), medium (orange) and low (blue) complexity of the image processing performed by the algorithm. In each frame, the panel is firstly detected and roughly segmented. That allows compensating the motion between different frames and register across all images of the sequence. After the denoising by averaging and BG subtraction steps, the
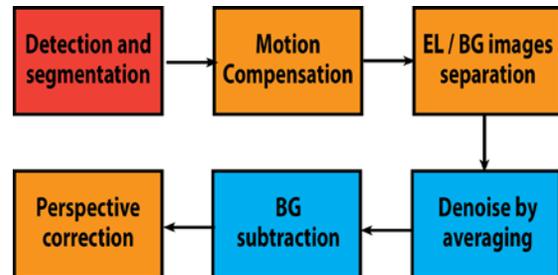
Figure 3: Diagram of image processing steps for daylight EL acquired in motion.

perspective deformation is corrected to obtain a perfectly square panel.

For accurate perspective distortion correction, the homography to determine, i.e. the transformation projecting the imaged PV panel back into the panel plan, has 8 degrees of freedom. As each corner of the PV panel determines two of those degrees of freedom, knowing the localization of the four corners of the considered panel allows to fully determining the homography parameters, which is done using the Direct Linear Transform (DLT) algorithm. The four corners are determined as the intersection of the four edges of the panel, themselves identified by rotating and projecting the image at various angles [9].

The computed motion compensation performed to align the module images is shown in Fig. 4, with "motion in the x" corresponding to the horizontal displacement and "motion in the y" corresponding to vibrations of the test bed construction. Vibrations are highly expected in a UAV
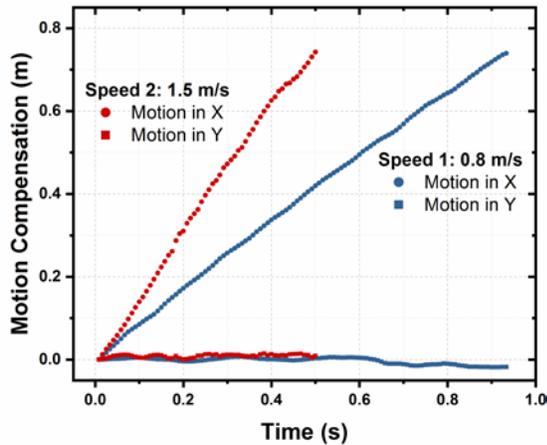
system specially if the flight is performed in windy conditions, hence the algorithm was prepared to cover this scenario.

Fig. 5 shows the mean of pixel numbers of the image sequences used for EL/BG separation at the two different speeds. The algorithm separates the images with a higher mean as EL images and lower mean as BG images, regardless of the curve shape observed. This curve shape indicates sun irradiance variations during the image acquisition (most likely due to clouds passing).

3.2 EL images

For comparison, Fig. 6 shows the stationary EL images acquired indoors in the dark (top) and outdoors under 849 W/m^2 at the POA (bottom). The outdoor EL image was

Figure 4: Motion compensation of EL images acquired in motion in two different speeds.
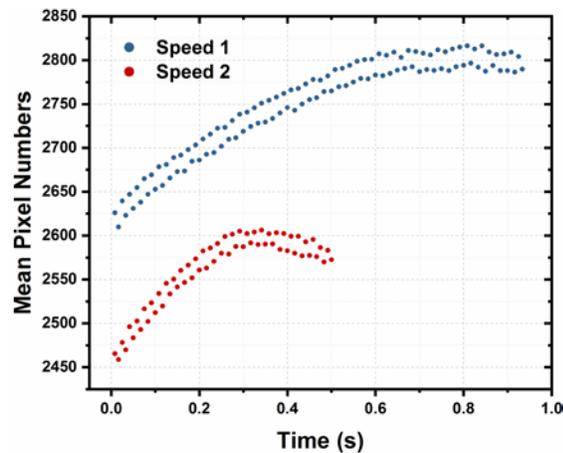
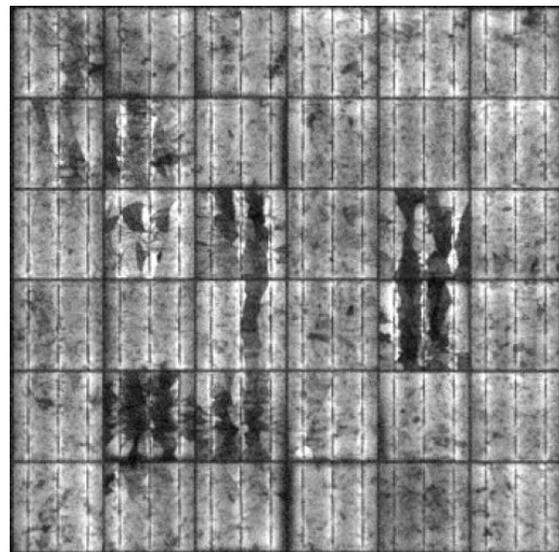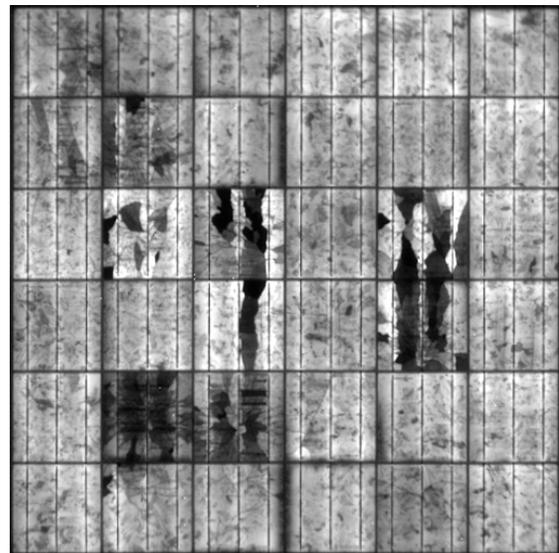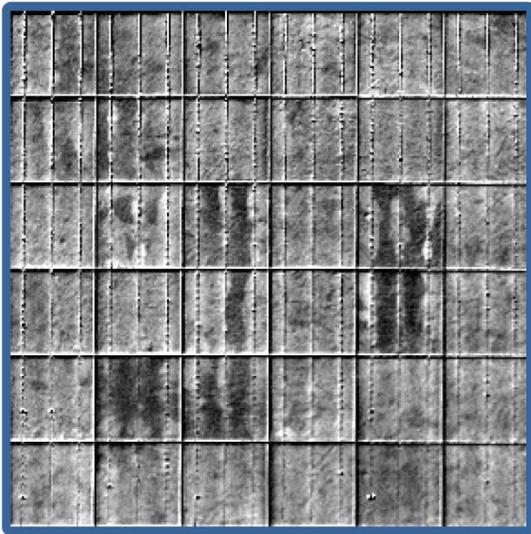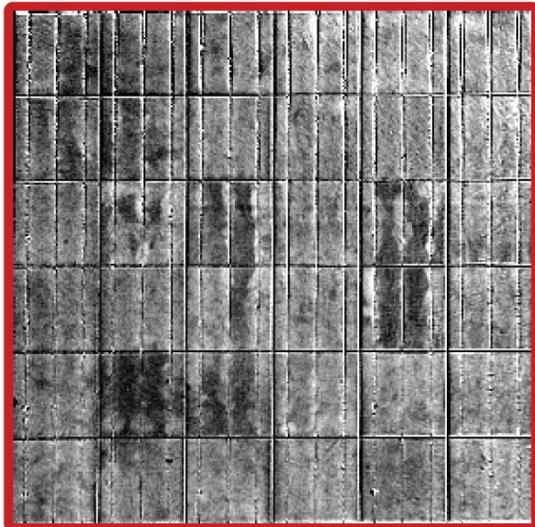**Figure 5:** Mean of pixel numbers of EL image sequences used for EL / BG separation.

Figure 6: Stationarry EL. Top: Indoors; bottom: Outdoors at 849 W/m^2 POA.

GHI: 775 W/m²
POA: 849 W/m²

Speed 1: 0.8 m/s

GHI: 761 W/m²
POA: 841 W/m²

Speed 2: 1.5 m/s

Figure 7: EL in motion. Top: Speed 1; Bottom: Speed 2.

obtained using EL/BG separation, denoise by averaging, BG subtraction and perspective correction image processing steps. The stationary outdoor image had $SNR_{50} > 5$ as recommended by the EL standard [10], where mode A, B and C cracks can be identified.

Fig. 7 shows the processed EL images acquired at speed 1 (top) and speed 2 (bottom). The images presented average quality, with B and C mode cracks well identified. No special treatment was required for the different speeds and the differences observed in the image alignment could be

observed in different sequences with similar speeds. The remaining misalignment, especially visible at the bus bar level, is due to perspective distortion as a result of changing viewpoint of the camera. This indicates the need to correct perspective distortion to all images separately first, before averaging and BG subtraction.

4   CONCLUSION AND OUTLOOK

We obtained in this work for the first time outdoor EL images of a PV panel with mode A, B and C cracks mounted in bright sunlight (> 800 W/m² in the POA) while the camera was in motion. The images obtained by motion compensation have an average quality, however it is still possible to recognize major cracks such as B and C cracks.

To improve from average to high image quality, the next step is to apply perspective correction to all acquired images separately and to register them better before averaging and subtraction. This new approach is challenging, as it needs the perspective correction to be perfectly robust across images. Additionally, the blur in EL images must be confirmed mathematically, especially for higher speeds in the future.

The application of such image corrections will support the development of UAV-based PV plant EL inspections in daylight, where each image has a different angular position from the camera viewpoint, and several images from each module have to be registered, averaged, and BG subtracted.

These results confirm the application of daylight measurement of lock-in EL in movement suggested by Adams et al. [5] and is a step further towards fast EL acquisition in the field.

5   ACKNOWLEDGEMENTS

6   REFERENCES

[1]   S. Dotenco *et al.*, "Automatic detection and analysis of photovoltaic modules in aerial infrared imagery," *2016 IEEE Winter Conf. Appl. Comput. Vis.*, pp. 1–9, 2016.

[2]   J. B. S. Koch, T. Weber, C. Sobottka, A. Fladung, P. Clemens, "Outdoor Electroluminescence Imaging of Crystalline Photovoltaic Modules: Comparative Study between Manual Ground-Level Inspections and Drone-Based Aerial Surveys," *32nd Eur. Photovolt. Sol. Energy Conf. Exhib.*, pp. 1736–1740, 2016.

[3]   M. Köntges *et al.*, "Review of Failures of Photovoltaic Modules," *IEA-Photovoltaic Power Syst. Program.*, pp. 1–140, 2014.

[4]   A.   Vision,   "Goldeye   CL-033,"

https://www.alliedvision.com/en/products/cameras/detail/Goldeye/CL-033 TEC1.html. .

[5]   J. Adams *et al.*, "Non-Stationary Outdoor EL-Measurements with a Fast and Highly Sensitive InGaAs Camera," *32nd Eur. Photovolt. Sol. Energy Conf. Exhib.*, 2016.

[6]   C. Buerhop and H. Scheuerpflug, "Field inspection of PV-modules using aerial, drone-mounted thermography," *29th Eur. Photovolt. Sol. Energy Conf. Exhib.*, pp. 2975–2979, 2013.

[7]   G. A. dos Reis Benatto *et al.*, "Development of outdoor luminescence imaging for drone-based PV array inspection," *44th IEEE Photovolt. Spec. Conf.*, 2017.

[8]   T. Fuyuki, H. Kondo, T. Yamazaki, Y. Takahashi, and Y. Uraoka, "Photographic surveying of minority carrier diffusion length in polycrystalline silicon solar cells by electroluminescence," *Appl. Phys. Lett.*, vol. 86, no. 26, pp. 1–3, 2005.

[9]   C. Mantel *et al.*, "Correcting for Perspective Distortion in Electroluminescence Images of Photovoltaic Panels," *IEEE 7th World Conf. Photovolt. Energy Convers.*, 2018.

[10]   IEC, "PNW/TS 82-901 Ed. 1.0 Photovoltaic Devices - Part 13: Electroluminescence of Photovoltaic Modules (proposed future IEC TS 60904-13)." http://www.iec.ch/.